J|A|C|S ARTICLES

Published on Web 08/10/2009

Critical Role of External Axial Ligands in Chirality Amplification of *trans*-Cyclohexane-1,2-diamine in Salen Complexes

Takuya Kurahashi,[†] Masahiko Hada,[‡] and Hiroshi Fujii*[,†]

Institute for Molecular Science and Okazaki Institute for Integrative Bioscience, National Institutes of Natural Sciences, Myodaiji, Okazaki, Aichi 444-8787, Japan, and Department of Chemistry, Graduate School of Science, Tokyo Metropolitan University, 1-1 Minami-Osawa, Hachioji-shi, Tokyo 192-0397, Japan

Received June 8, 2009; E-mail: hiro@ims.ac.jp

Abstract: A series of $Mn^{IV}(salen)(L)_2$ complexes bearing different external axial ligands (L = Cl, NO_3, N_3, and OCH_2CF_3) from chiral salen ligands with *trans*-cyclohexane-1,2-diamine as a chiral scaffold are synthesized, to gain insight into conformational properties of metal salen complexes. X-ray crystal structures show that $Mn^{IV}(salen)(OCH_2CF_3)_2$ and $Mn^{IV}(salen)(N_3)_2$ adopt a stepped conformation with one of two salicylidene rings pointing upward and the other pointing downward due to the bias from the *trans*-cyclohexane-1,2-diamine moiety, which is in clear contrast to a relatively planar solid-state conformation for $Mn^{IV}(salen)(Cl)_2$. The CH_2Cl_2 solution of $Mn^{IV}(salen)(L)_2$ shows circular dichroism of increasing intensity in the order L = Cl < NO_3 ≪ N_3 < OCH_2CF_3, which indicates $Mn^{IV}(salen)(L)_2$ adopts a solution conformation of an increasing chiral distortion in this order. Quantum-chemical calculations with a symmetry adapted cluster-configuration interaction method indicate that a stepped conformation exhibits more intense circular dichroism than a planar conformation. The present study clarifies an unexpected new finding that the external axial ligands (L) play a critical role in amplifying the chirality in *trans*-cyclohexane-1,2-diamine in $Mn^{IV}(salen)(L)_2$ to facilitate the formation of a chirally distorted conformation, possibly a stepped conformation.

Introduction

Salen ligands, which are diimine-diphenolate ligands bearing a linkage between two imine donors, have emerged as one of the most versatile synthetic ligands. Salen ligands, which are easily obtained by the condensation of a salicylaldehyde with a diamine, securely bind various metal ions in a tetradentate fashion. The malleability inherent to the salen ligand system has enabled access to metal centers with a wide variety of stereochemical and electronic properties and, thus, has led to their extensive use. Salen metal complexes are still expanding their utilities in catalysis,[1] in asymmetric synthesis,[2] in modeling enzymes,[3] in polymer synthesis,[4] in biological application,[5] and as synthons for supramolecular materials.[6]

The most promising feature of salen complexes is easily tunable stereochemical properties, including coordination geometries, conformations, and even supramolecular structures. It has been shown that coordination geometries as well as conformations could be modulated by changing a diamine linkage, leading to unique reactivity.[7−9] It has been also shown that salicylidene rings are appropriately modified for creating a chiral environment around the metal center, resulting in exquisite selectivity in asymmetric catalysis.[10] There is much current interest in constructing salen metal complexes with a helical motif, in which intramolecular hydrogen bonding, $\pi-\pi$ staking, and metal binding sites are rationally incorporated to the salicylidene rings to stabilize higher-order helical structures.[11−13] A recent intriguing example that makes use of fine-tuned

[†] National Institutes of Natural Sciences.
[‡] Tokyo Metropolitan University.

(1) (a) Atwood, D. A.; Harvey, M. J. *Chem. Rev.* **2001**, *101*, 37–52. (b) Cozzi, P. G. *Chem. Soc. Rev.* **2004**, *33*, 410–421.
(2) (a) Canali, L.; Sherrington, D. C. *Chem. Soc. Rev.* **1999**, *28*, 85–93. (b) Jacobsen, E. N. *Acc. Chem. Res.* **2000**, *33*, 421–431. (c) Bandini, M.; Cozzi, P. G.; Umani-Ronchi, A. *Chem. Commun.* **2002**, 919–927. (d) Irie, R.; Katsuki, T. *Chem. Rec.* **2004**, *4*, 96–109. (e) Katsuki, T. *Chem. Soc. Rev.* **2004**, *33*, 437–444. (f) McGarrigle, E. M.; Gilheany, D. G. *Chem. Rev.* **2005**, *105*, 1563–1602. (g) Baleizão, C.; Garcia, H. *Chem. Rev.* **2006**, *106*, 3987–4043. (h) Matsumoto, K.; Saito, B.; Katsuki, T. *Chem. Commun.* **2007**, 3619–3627.
(3) (a) Wu, A. J.; Penner-Hahn, J. E.; Pecoraro, V. L. *Chem. Rev.* **2004**, *104*, 903–938. (b) Costas, M.; Mehn, M. P.; Jensen, M. P.; Que, L., Jr. *Chem. Rev.* **2004**, *104*, 939–986.
(4) Darensbourg, D. J. *Chem. Rev.* **2007**, *107*, 2388–2410.
(5) (a) Muller, J. G.; Kayser, L. A.; Paikoff, S. J.; Duarte, V.; Tang, N.; Perez, R. J.; Rokita, S. E.; Burrows, C. J. *Coord. Chem. Rev.* **1999**, *185−186*, 761–774. (b) Thompson, K. H.; McNeill, J. H.; Orvig, C. *Chem. Rev.* **1999**, *99*, 2561–2571. (c) Riley, D. P. *Chem. Rev.* **1999**, *99*, 2573–2587.
(6) (a) Miyasaka, H.; Saitoh, A.; Abe, S. *Coord. Chem. Rev.* **2007**, *251*, 2622–2664. (b) Wezenberg, S. J.; Kleij, A. W. *Angew. Chem., Int. Ed.* **2008**, *47*, 2354–2364. (c) Kleij, A. W. *Chem.—Eur. J.* **2008**, *14*, 10520–10529.
(7) Wang, Y.; DuBois, J. L.; Hedman, B.; Hodgson, K. O.; Stack, T. D. P. *Science* **1998**, *279*, 537–540.
(8) Hormnirun, P.; Marshall, E. L.; Gibson, V. C.; Pugh, R. I.; White, A. J. P. *Proc. Natl. Acad. Sci. U.S.A.* **2006**, *103*, 15343–15348.
(9) Kim, H.-J.; Kim, W.; Lough, A. J.; Kim, B. M.; Chin, J. *J. Am. Chem. Soc.* **2005**, *127*, 16776–16777.
(10) Watanabe, A.; Uchida, T.; Irie, R.; Katsuki, T. *Proc. Natl. Acad. Sci. U.S.A.* **2004**, *101*, 5737–5742.
(11) Dong, Z.; Karpowicz, R. J., Jr.; Bai, S.; Yap, G. P. A.; Fox, J. M. *J. Am. Chem. Soc.* **2006**, *128*, 14242–14243.
(12) Wiznycia, A. V.; Desper, J.; Levy, C. J. *Inorg. Chem.* **2006**, *45*, 10034–10036.

10.1021/ja904635n CCC: $40.75

Chart 1. Salen Ligands That Are Utilized in This Study

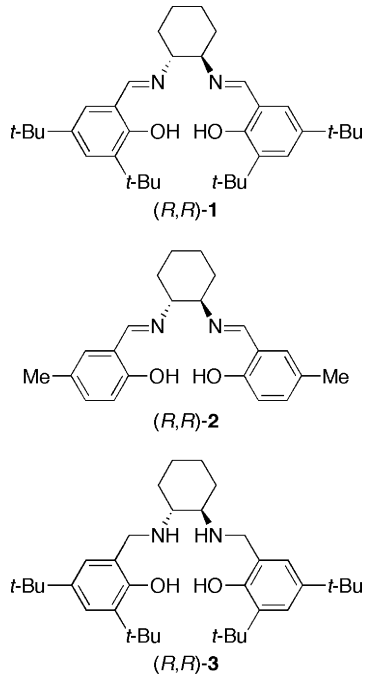

stereochemical properties is a salen-based supramolecule that shows a solvent-dependent transformation between a triangular macrocycle and a helical coordination polymer.[14]

Among salen ligands reported so far, (*R*,*R*)- or (*S*,*S*)-*N*,*N*′-bis(3,5-di-*tert*-butylsalicylidene)-1,2-cyclohexanediamine (**1**, Chart 1), which was developed by Jacobsen and co-workers, is now known as one of the "privileged chiral ligands", and metal complexes from **1** show high levels of enantioselectivity for mechanistically unrelated reactions such as epoxidation of olefins, ring-opening reaction of epoxides, and conjugate addition of azide to unsaturated imides.[15] In spite of outstanding enantioselectivity generally seen for Jacobsen's catalyst, the origins of enantioselectivity are not fully understood and still remain to be the subject of active research.[2f,16−19] The conformational properties of these chiral catalysts are of prime importance, but very few studies on this subject have been reported.[16,18] Jacobsen's ligand **1** possesses a *trans*-cyclohexane-1,2-diamine linkage as the only chiral unit and salicylidene rings modified by sterically demanding *tert*-butyl groups. Although the C_2 symmetrical *trans*-cyclohexane-1,2-diamine scaffold in enantiopure form has served as a powerful stereodirecting group for creating chiral molecular architechtures,[20] X-ray structural studies by Jacobsen et al. show that salen metal complexes from **1** usually adopt an almost planar structure and the *tert*-butyl groups incorporated to the salicylidene rings are not bulky enough to induce distortion of the planar N_2O_2 coordination geometry.[21] Nevertheless, it has been frequently proposed that a subtle deviation from planarity of the conformation of these catalysts is critically important in determining the course of asymmetric reactions.[2f] Among very few studies on conformational properties, Chin et al. reported intriguing X-ray structures for the Co^{III}(salen) complexes from (*R*,*R*)- and (*S*,*S*)-**1** that bind two chiral aziridine molecules as a transition-state analogue for enantioselective epoxidation of olefins or ring-opening reactions of epoxides.[16] They found the salicylidene rings in Co^{III}(salen)(aziridine)$_2$ complexes are considerably distorted from planarity, which they claim is responsible for the different binding affinity between the Co^{III}(salen) complexes from (*R*,*R*)- and (*S*,*S*)-**1** for the chiral aziridine in solution. In contrast, Fox et al. recently pointed out that the distortion of the salicylidene rings that is directed by *trans*-cyclohexane-1,2-diamine is unexpectedly small, by rigorously studying the solution conformations of their well-designed Ni^{II}(salen) complexes.[18]

Our continuing interest in higher-valent intermediates from salen complexes[22] and the quite puzzling conformational properties of Jacobsen's salen complexes prompted us to study conformations of higher-valent Mn(salen) complexes from **1**. We recently reported a preparation of Mn^{IV}(salen)$(N_3)_2$ from **1**, a rare example of a monomeric high-valent Mn^{IV} complex in the salen platform.[23] An X-ray crystal structure of Mn^{IV}(salen)$(N_3)_2$ from (*R*,*R*)-**1** adopts a nonplanar stepped conformation with one of two salicylidene rings pointing upward and the other pointing downward, although the one-electron reduced Mn^{III}(salen)$(N_3)(CH_3OH)$ exhibits a planar structure. To gain further understanding, we herein prepare and fully characterize monomeric Mn^{IV}(salen)$(L)_2$ bearing different external axial ligands (L = Cl, NO_3, and OCH_2CF_3) from (*R*,*R*)-**1** and investigate their solid-state and solution conformations by means of X-ray crystallography, circular dichroism, and ^{2}H NMR (nuclear magnetic resonance) spectroscopy, with the help of quantum-chemical calculations. Quite interestingly, Mn^{IV}(salen)$(L)_2$ is shown to adopt a solution conformation of an increasing chiral distortion in the order L = Cl < NO_3 ≪ N_3 < OCH_2CF_3. The present study clarifies an unexpected new finding that the external axial ligands (L) play a critical role in amplifying the chirality in *trans*-cyclohexane-1,2-diamine in Mn^{IV}(salen)$(L)_2$ to facilitate the formation of a chirally distorted conformation, possibly a stepped conformation.

Results

Synthesis and Characterization of Mn^{IV}(salen)$(L)_2$ from Jacobsen's Ligand and a Salen Ligand with Less Steric Bulk. As summarized in Scheme 1, we prepared new Mn^{IV}(salen)$(L)_2$ from (*R*,*R*)-**1**, which are denoted as **1**-L (where L = Cl, NO_3, N_3,[23] and OCH_2CF_3). We also prepared Mn^{IV}(salen)$(N_3)_2$ from (*R*,*R*)-*N*,*N*′-bis(5-methylsalicylidene)-1,2-cyclohexanediamine ((*R*,*R*)-**2**, Chart 1) with less steric bulk, which is denoted as **2**-N_3. The stream of O_3 and O_2 prepared by UV-irradiation to the O_2 gas was passed through the CH_2Cl_2

(13) Akine, S.; Taniguchi, T.; Nabeshima, T. *J. Am. Chem. Soc.* **2006**, *128*, 15765–15774.
(14) Heo, J.; Jeon, Y.-M.; Mirkin, C. A. *J. Am. Chem. Soc.* **2007**, *129*, 7712–7713.
(15) Yoon, T. P.; Jacobsen, E. N. *Science* **2003**, *299*, 1691–1693.
(16) Bobb, R.; Alhakimi, G.; Studnicki, L.; Lough, A.; Chin, J. *J. Am. Chem. Soc.* **2002**, *124*, 4544–4545.
(17) (a) Fallis, I. A.; Murphy, D. M.; Willock, D. J.; Tucker, R. J.; Farley, R. D.; Jenkins, R.; Strevens, R. R. *J. Am. Chem. Soc.* **2004**, *126*, 15660–15661. (b) Murphy, D. M.; Fallis, I. A.; Willock, D. J.; Landon, J.; Carter, E.; Vinck, E. *Angew. Chem., Int. Ed.* **2008**, *47*, 1414–1416.
(18) Dong, Z.; Yap, G. P. A.; Fox, J. M. *J. Am. Chem. Soc.* **2007**, *129*, 11850–11853.
(19) Kemper, S.; Hrobárik, P.; Kaupp, M.; Schlörer, N. E. *J. Am. Chem. Soc.* **2009**, *131*, 4172–4173.
(20) Bennani, Y. L.; Hanessian, S. *Chem. Rev.* **1997**, *97*, 3161–3195.
(21) (a) Pospisil, P. J.; Carsten, D. H.; Jacobsen, E. N. *Chem.—Eur. J.* **1996**, *2*, 974–980. (b) Hansen, K. B.; Leighton, J. L.; Jacobsen, E. N. *J. Am. Chem. Soc.* **1996**, *118*, 10924–10925. (c) Ready, J. M.; Jacobsen, E. N. *J. Am. Chem. Soc.* **1999**, *121*, 6086–6087.
(22) (a) Kurahashi, T.; Kobayashi, Y.; Nagatomo, S.; Tosha, T.; Kitagawa, T.; Fujii, H. *Inorg. Chem.* **2005**, *44*, 8156–8166. (b) Kurahashi, T.; Kikuchi, A.; Tosha, T.; Shiro, Y.; Kitagawa, T.; Fujii, H. *Inorg. Chem.* **2008**, *47*, 1674–1686.
(23) Kurahashi, T.; Fujii, H. *Inorg. Chem.* **2008**, *47*, 7556–7567.

Scheme 1

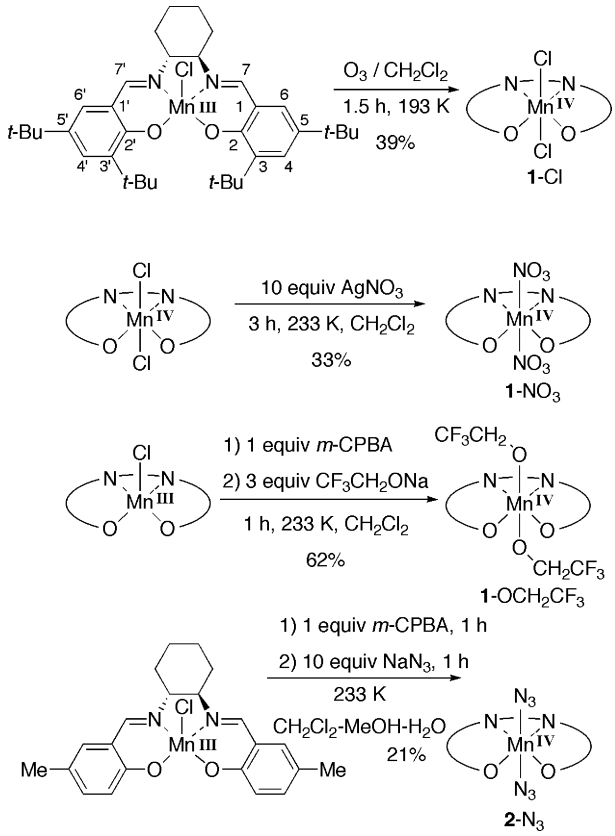

solution of Mn^{III}(salen)(Cl) from (*R*,*R*)-**1** at 193 K to give **1**-Cl as a green powdery sample. **1**-Cl dissolved in CH_2Cl_2 is stable at room temperature for hours. **1**-NO_3 was prepared as a green solid by the reaction of **1**-Cl with 10 equiv of $AgNO_3$ in CH_2Cl_2 for 3 h at 233 K. **1**-NO_3 in CH_2Cl_2 decomposes at room temperature ($t_{1/2} \approx 20$ min). **1**-OCH_2CF_3 was prepared as a brown solid by oxidation of Mn^{III}(salen)(Cl) from (*R*,*R*)-**1** with 1.0 equiv of *m*-CPBA (*m*-chloroperoxybenzoic acid) and a subsequent ligand exchange by addition of 3 equiv of CF_3CH_2ONa. **1**-OCH_2CF_3 in CH_2Cl_2 is stable at room temperature for hours. Reaction of Mn^{III}(salen)(Cl) from (*R*,*R*)-**2** at 233 K with 1 equiv of *m*-CPBA and a subsequent ligand exchange by addition of 10 equiv of NaN_3 gave **2**-N_3 as a green solid. Repeated precipitation in CH_2Cl_2−pentane at 233 K three times gave an analytically pure sample. **2**-N_3 in CH_2Cl_2 slowly decomposes at room temperature ($t_{1/2} \approx 2$ h).

To confirm that **1**-L and **2**-N_3 have a Mn^{IV} center, EPR (electron paramagnetic resonance) spectra are measured at 4 K. The EPR spectrum of **1**-OCH_2CF_3 at 4 K in Figure 1a exhibits signals at $g = 3.56$ and 2.00, which are typical of an $S = {}^3/_2$ spin system ($E/D \approx 0$) from d^3 Mn^{IV}.[22b,23,24] The signal at $g = 2.00$ displays a six-line hyperfine splitting due to the $I = {}^5/_2$ ^{55}Mn nucleus. **1**-NO_3 shows one set of EPR signals at $g = 5.04$, 2.96, and 1.83 along with a weak signal at $g = 5.63$ (Figure 1b), which are also typical of an $S = {}^3/_2$ spin system ($E/D \approx 0.25$) from d^3 Mn^{IV}.[22b,23,24] The signals at $g = 5.04$, 2.96, and 1.83 arise from the $m_s = \pm{}^1/_2$ doublets,

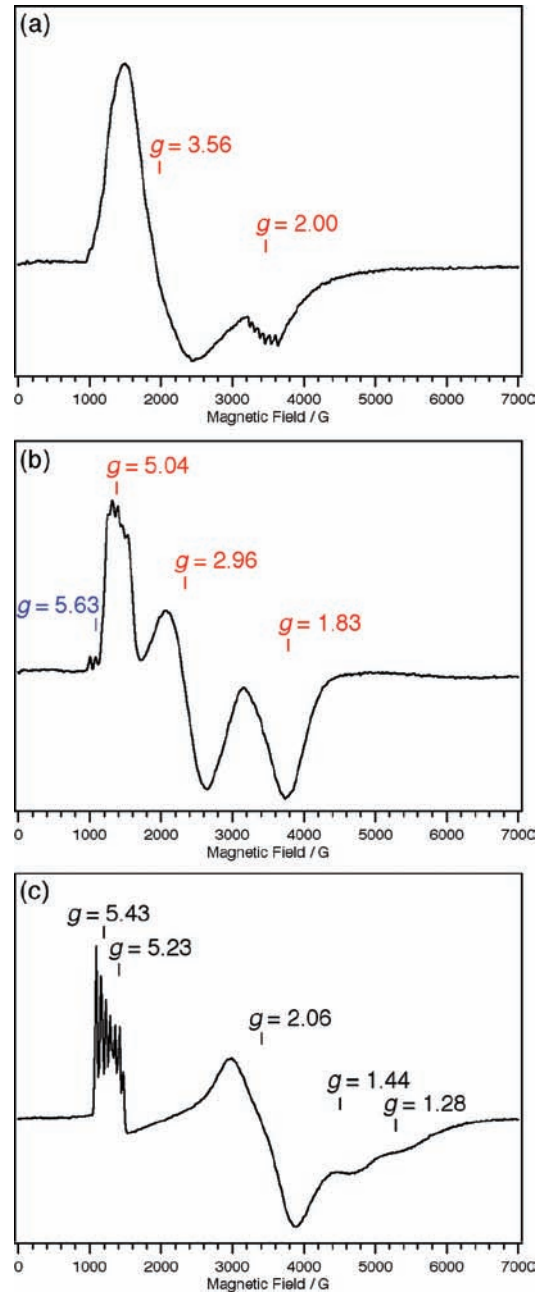

Figure 1. X-band EPR spectra of (a) **1**-OCH_2CF_3, (b) **1**-NO_3, and (c) **1**-Cl in frozen CH_2Cl_2−toluene (7:3) at 4 K. Signals that arise from $m_s = \pm{}^1/_2$ and $\pm{}^3/_2$ doublets of $S = {}^3/_2$ are written in red and blue, respectively. Magnetic parameters: (a) $E/D \approx 0$, (b) $E/D \approx 0.25$, (c) E/D not determined. Conditions: microwave frequency, 9.56 GHz; microwave power, 2.012 mW; modulation amplitude, 7 G; time constant, 163.84 ms; conversion time, 163.84 ms.

and the weak signal at $g = 5.63$ arises from the $m_s = \pm{}^3/_2$ doublets of an $S = {}^3/_2$ spin system. **1**-Cl exhibits intense EPR signals shown in Figure 1c, which is consistent with the assignment as a mononuclear Mn^{IV} complex. The EPR spectrum of **1**-Cl contains multiple sets of signals, which may indicate multiple Mn^{IV} species with different rhombicity in solution or could be alternatively interpreted as arising from the $m_s = \pm{}^1/_2$ and $m_s = \pm{}^3/_2$ doublets from a single Mn^{IV} species. **2**-N_3 shows EPR signals that are typical of an $S = {}^3/_2$ spin system ($E/D \approx 0$) from d^3 Mn^{IV} (Figure S1, Supporting Information).

(24) (a) Bryliakov, K. P.; Babushkin, D. E.; Talsi, E. P. *J. Mol. Catal. A* **2000**, *158*, 19–35. (b) Adam, W.; Mock-Knoblauch, C.; Saha-Möller, C. R.; Herderich, M. *J. Am. Chem. Soc.* **2000**, *122*, 9685–9691. (c) Campbell, K. A.; Lashley, M. R.; Wyatt, J. K.; Nantz, M. H.; Britt, R. D. *J. Am. Chem. Soc.* **2001**, *123*, 5710–5719.

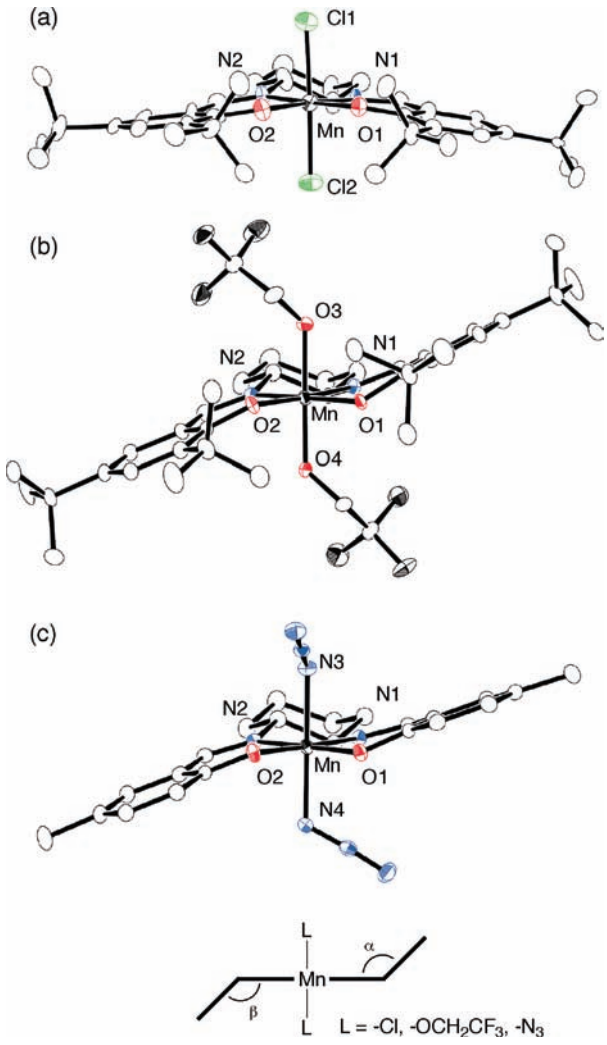

Figure 2. X-ray crystal structures of (a) **1**-Cl, (b) **1**-OCH_2CF_3, and (c) **2**-N_3. Thermal ellipsoids represent the 50% probability surfaces. Hydrogen atoms and a disordered *tert*-butyl group in **1**-OCH_2CF_3 are omitted for the sake of clarity. The angles α and β are defined as those between the planes of the salicylidene rings and the least-squares plane of the N_2O_2 of the salen ligand.

X-ray Crystal Structures of 1-Cl, 1-OCH_2CF_3, and 2-N_3. X-ray crystal structures of **1**-Cl, **1**-OCH_2CF_3, and **2**-N_3 were successfully determined (Figure 2), although we could not obtain a crystal of **1**-NO_3 that is suitable for the X-ray crystallography. Table 1 summarizes the crystallographic data. The asymmetric unit of **1**-Cl contains two mononuclear complexes. One is shown in Figure 2a, and the other is included in the Supporting Information (Figure S3). The asymmetric unit of **1**-OCH_2CF_3 and that of **2**-N_3 contain one mononuclear complex, which is shown in Figure 2b and 2c, respectively. As shown in the packing diagrams (Figure S2, Supporting Information), the intermolecular Mn−Mn distances in the unit cell of **1**-Cl and **2**-N_3 is 7.43 and 7.61 Å, respectively, while that of **1**-OCH_2CF_3 is longer (16.26 Å), due to the steric bulk of the CF_3CH_2O groups incorporated to the axial coordination sites. Table 2 compiles selected structural parameters. Table 2 also includes parameters α and β, which are defined as angles between the planes of the salicylidene rings and the least-squares plane of the N_2O_2 of the salen ligand,[2f] as shown in Figure 2.

X-ray crystal structures in Figure 2 show all the Mn^{IV}(salen) complexes have a planar N_2O_2 equatorial coordination sphere with external ligands that occupy axial coordination sites.

Table 1. Crystallographic Data for **1**-Cl, **1**-OCH_2CF_3, and **2**-N_3

	1-Cl	**1**-OCH_2CF_3	**2**-N_3
formula	$C_{76}H_{112}Cl_{12}Mn_2N_4O_4$	$C_{44}H_{62}F_6MnN_4O_4$	$C_{22}H_{24}MnN_8O_2$
M_r	1681.06	879.92	487.42
T/K	93	93	93
cryst size/mm^3	0.20 × 0.15 × 0.15	0.30 × 0.25 × 0.05	0.30 × 0.20 × 0.05
cryst syst	triclinic	monoclinic	orthorhombic
space group	$P1$ (No. 1)	$P2_1$ (No. 4)	$P2_12_12_1$ (No. 19)
cryst color	dark red	black	brown
λ/Å	0.710 70	0.710 70	0.710 70
μ/mm^{-1}	0.746	0.355	0.616
a/Å	12.628(4)	9.671(2)	8.5312(4)
b/Å	12.917(5)	23.135(5)	13.4133(7)
c/Å	14.498(6)	10.267(2)	19.9001(10)
α/deg	82.04(3)	90.0000(14)	90.0000
β/deg	73.07(2)	95.5892(15)	90.0000
γ/deg	65.24(2)	90.0000(14)	90.0000
V/Å^3	2053.9(13)	2286.1(8)	2277.20(20)
Z value	1	2	4
D_{calc}/g cm^{-3}	1.359	1.275	1.422
GOF	1.093	0.897	1.095
R_1[a]	0.0842	0.0499	0.0381
R_w[b]	0.2474	0.1418	0.0946
Flack	0.04(5)	0.057(15)	0.027(15)

[a] $R_1 = \Sigma||F_o| - |F_c||/\Sigma|F_o|$. [b] $R_w = [\Sigma w(F_o^2 - F_c^2)^2/\Sigma w(F_o^2)^2]^{1/2}$.

Table 2. Selected Structural Parameters for **1**-Cl, **1**-OCH_2CF_3, and **2**-N_3

	1-Cl[a]	**1**-Cl[b]	**1**-OCH_2CF_3	**2**-N_3
α/deg	191.4	154.5	154.7	158.5
β/deg	173.6	170.3	158.7	160.9
Mn−N_2O_2 plane/Å	0.023	0.017	0.009	0.005
Mn−O1/Å	1.867(10)	1.847(10)	1.873(2)	1.8546(16)
Mn−O2/Å	1.844(8)	1.857(8)	1.873(2)	1.8522(16)
Mn−N1/Å	1.992(8)	1.965(8)	1.986(2)	1.9775(19)
Mn−N2/Å	1.971(11)	1.988(11)	1.986(2)	1.9912(17)
Mn−L[c]/Å	2.300(2)	2.270(2)	1.880(2)	1.992(2)
Mn−L[c]/Å	2.263(2)	2.283(2)	1.866(2)	1.9836(19)
O1−C2/Å	1.321(16)	1.334(15)	1.329(3)	1.329(2)
O2−C2′/Å	1.316(18)	1.325(16)	1.329(3)	1.334(2)
N1−C7/Å	1.292(19)	1.297(17)	1.281(4)	1.286(2)
N2−C7′/Å	1.277(19)	1.295(18)	1.286(4)	1.286(2)
C1−C7/Å	1.415(19)	1.458(17)	1.445(4)	1.446(3)
C1′−C7′/Å	1.453(17)	1.404(14)	1.440(4)	1.445(3)
O1−Mn−N2/deg	174.6(3)	172.0(3)	173.56(9)	175.07(7)
O2−Mn−N1/deg	172.8(4)	173.6(4)	173.43(9)	175.47(7)

[a] Shown in Figure 2a. [b] Shown in Figure S3 (Supporting Information). [c] L denotes Cl, OCH_2CF_3, or N_3.

1-OCH_2CF_3 adopts a stepped conformation,[25] which is similar to that of **1**-N_3.[23] **2**-N_3 with less steric bulk also adopts a stepped conformation, clearly indicating sterically demanding *tert*-butyl groups in (*R*,*R*)-**1** are not an indispensable prerequisite for the formation of a chirally distorted stepped conformation. Notably, the conformation of **1**-Cl is much less distorted. As summarized in Table 2, **1**-OCH_2CF_3 and **2**-N_3 in a stepped conformation bears shorter Mn−OCH_2CF_3 bonds (1.866 and 1.880 Å) and Mn−N_3 bonds (1.992 and 1.984 Å), while less-distorted **1**-Cl bears considerably longer Mn−Cl bonds (2.263−2.300 Å). But the other structural parameters, including Mn−O_{salen} and Mn−N_{salen} bonds, are quite similar for all the Mn^{IV}(salen) complexes.

Solution Studies of 1-L. Solution conformations of the Mn^{IV}(salen) complexes are investigated by means of CD (circular dichroism) spectroscopy. For the purpose of assigning the CD bands from the ligand moiety of Mn(salen), we first measured the UV−vis and CD spectra of the salen ligand

(25) For proposed conformations of Mn(salen), see ref 2f.

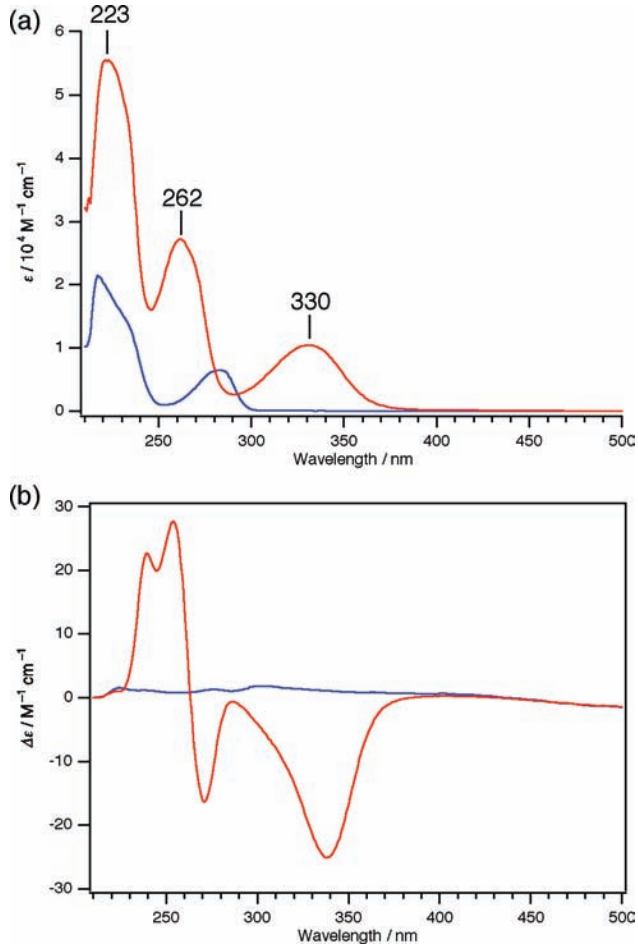

Figure 3. (a) UV−vis and (b) CD spectra of (*R*,*R*)-**1** (red line) and (*R*,*R*)-**3** (blue line) in CH_2Cl_2 (0.6 mM) at room temperature.

(*R*,*R*)-**1** and the tetrahydrosalen ligand (*R*,*R*)-**3** (Chart 1). (*R*,*R*)-**1** exhibits three UV−vis absorptions and the corresponding three CD bands in the region 200−400 nm (Figure 3). It is thus expected that Mn^{IV}(salen) complexes may also exhibit ligand-derived UV−vis absorptions and CD bands in this region. In contrast, (*R*,*R*)-**3** without the azomethine moiety exhibits only two UV−vis absorptions suggesting one of three UV−vis absorptions in (*R*,*R*)-**1** might be assigned as originating from the azomethine moiety, while the other two might originate from the phenolates. It is interesting to note that (*R*,*R*)-**3** shows negligibly weak CD as compared to (*R*,*R*)-**1**,[26] suggesting the azomethine moiety plays a role in inducing relatively strong CD in (*R*,*R*)-**1**.

Figure 4 shows UV−vis spectra of **1**-L (L = Cl, NO_3, N_3,[23] and OCH_2CF_3). All the Mn^{IV}(salen) complexes commonly exhibit two UV−vis absorptions of similar intensity in the region 200−300 nm. These are most probably derived from the salen ligand, in comparison with the UV−vis spectrum of (*R*,*R*)-**1** shown in Figure 3. Another remarkable feature is the absorption at >600 nm, which is shifted by substitution of the axial ligand L. In the case of **1**-OCH_2CF_3, the corresponding absorption may be shifted to the region of <600 nm. These absorptions are most probably assigned as the phenolate-to-Mn^{IV} charge transfer band. **1**-N_3 exhibits an absorption at 439 nm, which was previously assigned as the N_3-to-Mn^{IV} charge transfer band.[23]

(26) Weak CD for (*R*,*R*)-**3** is not due to racemization during the preparation, because (*S*,*S*)-**3** shows CD of the opposite sign to (*R*,*R*)-**3** (Figure S4, Supporting Information).

Figure 5 shows CD spectra of **1**-L (L = Cl, NO_3, N_3,[23] and OCH_2CF_3) under exactly the same measurement conditions. The intensity of CD in the region 200−300 nm, which is derived from the salen ligand, is considerably increased in the order L = Cl < NO_3 ≪ N_3 < OCH_2CF_3. Because the UV−vis absorptions in this region do not differ in intensity for all the (*R*,*R*)-Mn^{IV}(salen) complexes, the CD change in this region is solely ascribed to a conformational difference, rather than an overlap with additional CD upon substitution of the axial ligands. CD spectroscopy thus indicates **1**-OCH_2CF_3 and **1**-N_3 in solution adopt a conformation in which the salen ligand is more chirally distorted, as compared to **1**-Cl and **1**-NO_3. This is nicely in accord with the observation in the solid state, which shows both **1**-OCH_2CF_3 and **1**-N_3 adopt a chirally distorted stepped conformation, in contrast to a relatively planar conformation for **1**-Cl. **2**-N_3 with less steric bulk also exhibits a much more intense CD as compared with the starting Mn^{III}(salen)(Cl) in the region 200−300 nm (Figure S5, Supporting Information), indicating **2**-N_3, which is crystallized as a stepped conformation, also adopts a chirally distorted conformation in solution. Further insight into the chiroptical properties was obtained from variable-temperature CD measurements for **1**-OCH_2CF_3 and **1**-Cl (Figure 6). As the temperature of the sample solution is decreased from 293 to 233 K, all the CD bands of **1**-OCH_2CF_3 are increased. The same is true for **1**-N_3 as reported previously.[23] This is indicative of an equilibrium between a chirally distorted conformation at a lower energy level and a less chirally distorted conformation at a higher energy level for **1**-OCH_2CF_3 and **1**-N_3. In contrast, in the case of **1**-Cl, CD in the region 300−500 nm is increased upon cooling the sample solution, but CD in the region 200−300 nm, which reflects conformational changes of the salen ligand, is not altered. The absence of the temperature-dependent CD change in the region 200−300 nm for **1**-Cl may suggest every conformation that **1**-Cl may adopt is at a similar energy level.

Solution conformations of **1**-L were also investigated with NMR spectroscopy. Due to the paramagnetic high-spin d^3 Mn^{IV} center, Mn^{IV}(salen) complexes show multiple ^1H NMR signals at largely shifted positions.[22b,23,24a,27] As shown in Figure S6 (Supporting Information), **1**-L commonly exhibits three downfield-shifted signals and two upfield-shifted signals, except for **1**-NO_3 that exhibits an additional signal at −40.4 ppm. For the purpose of assignment of these signals, we employed ^2H NMR for ^2H-labeled salen complexes. A ^2H-labeled Jacobsen's salen ligand, (*R*,*R*)-**1**-*d*, was prepared from phenol-d_6. ^1H and ^2H NMR indicate that ^2H atoms are selectively incorporated to the phenolate rings (80% D) as well as the *tert*-butyl groups (7% D) in (*R*,*R*)-**1**-*d* (Figure S7, Supporting Information). As clearly seen from ^2H NMR spectra in Figure 7, **1**-L-*d* commonly exhibits one downfield-shifted and one upfield-shifted signal, which are unambiguously assigned as arising from the 4/4′H and 6/6′H of the phenolate rings (for numbering of the aromatic rings, see Scheme 1).[28] Then, the signals within the diamagnetic region are assigned as arising from the *tert*-butyl groups. Since the paramagnetic shifts of the *tert*-butyl groups are mainly induced by dipolar magnetic interaction, a broad signal that is more shifted could be assigned as arising from the *tert*-butyl groups at 3/3′ positions close to the paramagnetic Mn center,

(27) Bonadies, J. A.; Maroney, M. J.; Pecoraro, V. L. *Inorg. Chem.* **1989**, *28*, 2044–2051.

(28) We had incorrectly assigned the ^1H NMR signals from **1**-N_3 in our previous report,[23] which leads to an incorrect interpretation that two phenolate rings in **1**-N_3 are not equivalent in solution.

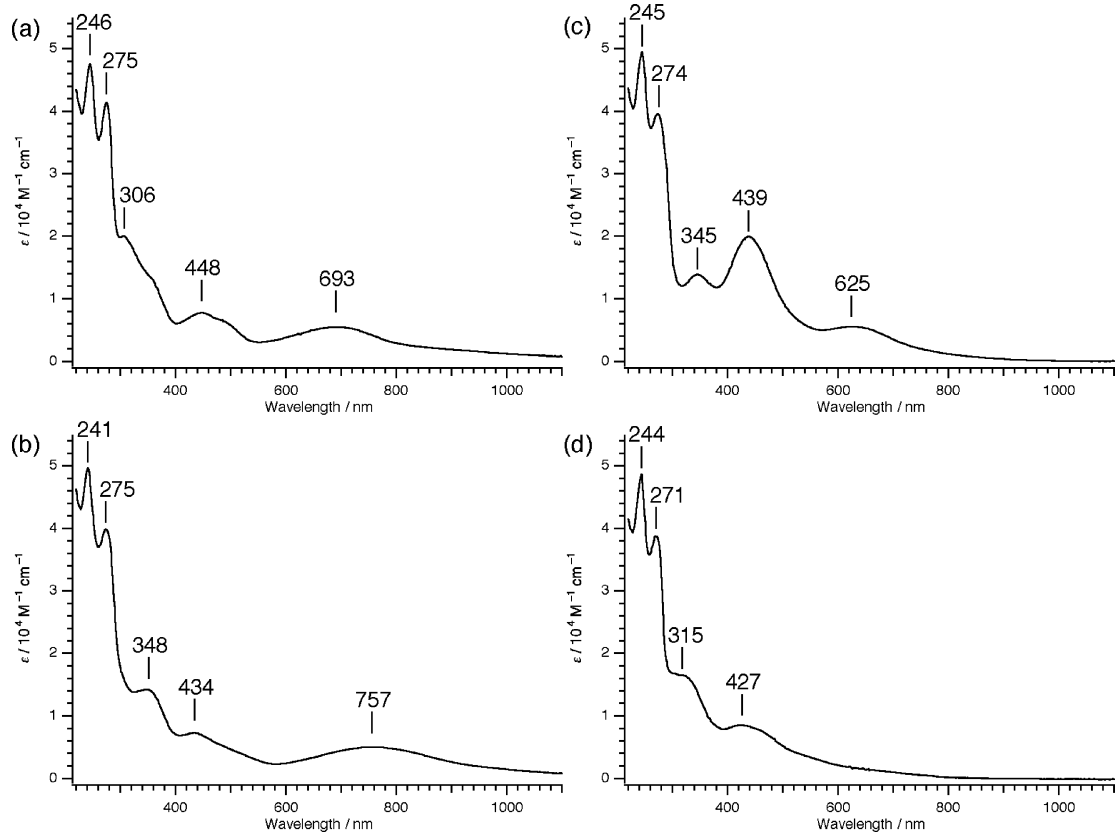

Figure 4. UV−vis spectra of (a) **1**-Cl, (b) **1**-NO_3, (c) **1**-N_3, and (d) **1**-OCH_2CF_3 in CH_2Cl_2 (0.3 mM) at 233 K.

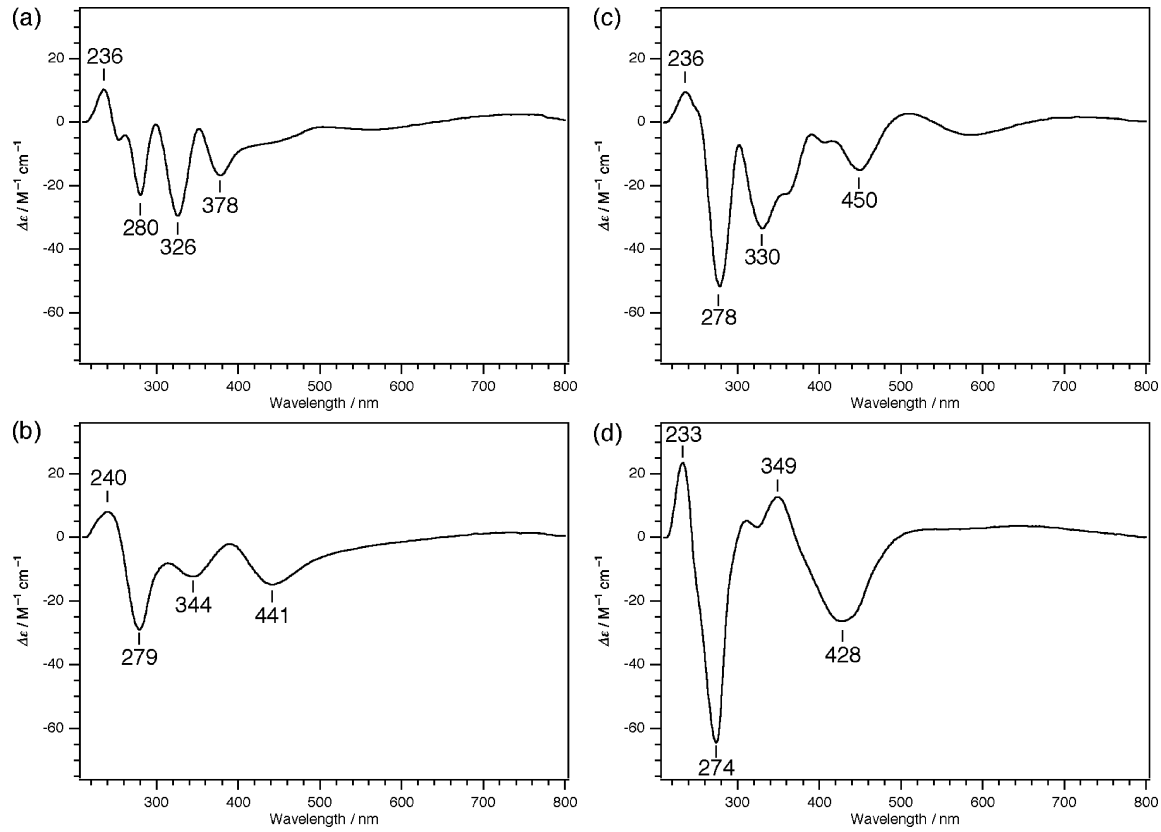

Figure 5. Circular dichroism spectra of (a) **1**-Cl, (b) **1**-NO_3, (c) **1**-N_3, and (d) **1**-OCH_2CF_3 in CH_2Cl_2 (0.3 mM) at 233 K.

while the other sharp signal could be assigned as arising from the *tert*-butyl groups at 5/5′ positions, which are more distant from the Mn center. ^{1}H NMR signals at approximately −40 ppm and <20 ppm could be tentatively assigned as arising from

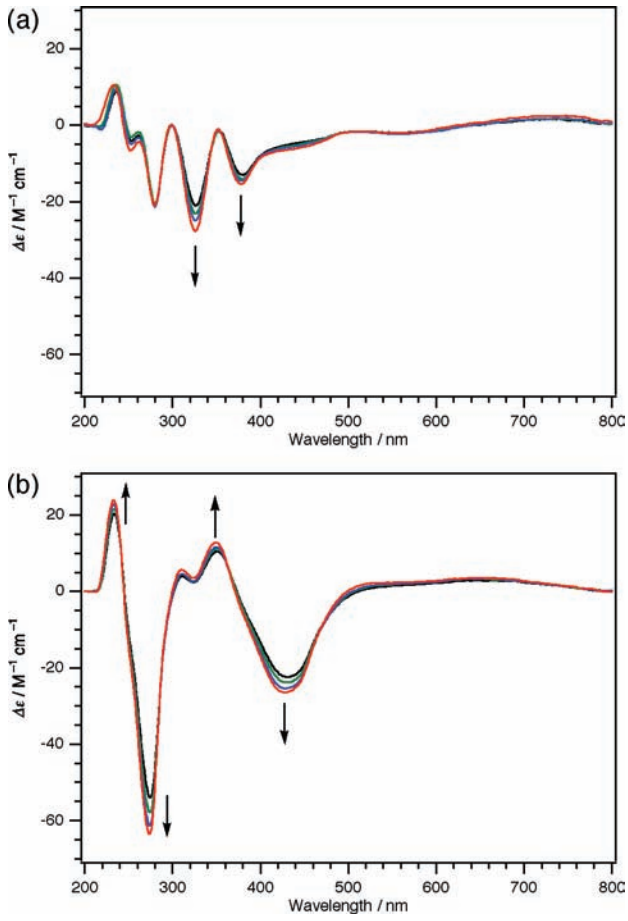

Figure 6. Circular dichroism spectra of (a) **1**-Cl and (b) **1**-OCH_2CF_3 in CH_2Cl_2 (0.3 mM) at 293 (black line), 273 (green line), 253 (blue line), and 233 K (red line).

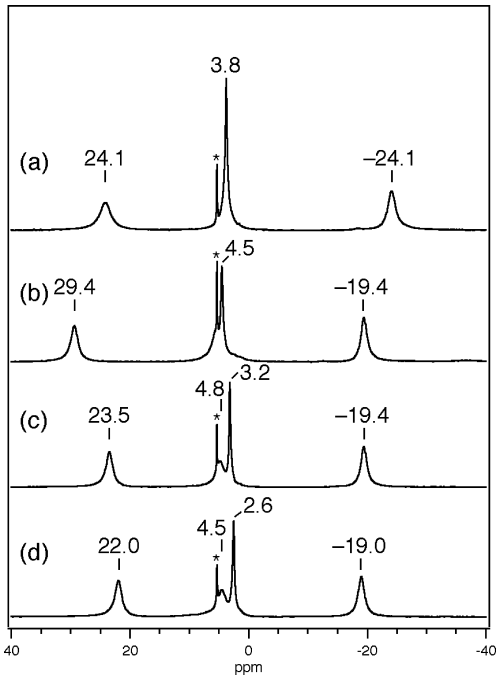

Figure 7. ^{2}H NMR (76.65 MHz) spectra of (a) **1**-Cl-*d*, (b) **1**-NO_3-*d*, (c) **1**-N_3-*d*, and (d) **1**-OCH_2CF_3-*d* in CH_2Cl_2 (40 mM) at 233 K. The signal designated with an asterisk comes from residual $CHDCl_2$ and is referenced to 5.32 ppm.

the azomethine proton and from the cyclohexane protons, respectively, based on the spin polarization mechanism from Mn^{IV} center.

As shown in Figure 7, ^{2}H NMR signals for the 4/4′H and 6/6′H of the phenolate rings in **1**-L-*d* appear outside the normal diamagnetic region, due to the paramagnetic effect from the Mn center through the π-system of the salen ligand. Paramagnetic shifts of the 4/4′H and 6/6′H of the phenolate rings in **1**-L-*d* increase in the order L = OCH_2CF_3 < N_3 ≪ NO_3 ≈ Cl. This might be partly due to a difference in interaction between the Mn *d*-orbital and the phenolate π-orbital; the paramagnetic shift would be decreased with the distortion of the phenolate rings from the planar conformation. Another point to be noted is a ^{2}H NMR signal from the *tert*-butyl groups at 5/5′ positions, which shows increasing paramagnetic shifts in the order L = OCH_2CF_3 < N_3 < Cl < NO_3. Paramagnetic shifts of the *tert*-butyl groups via a dipolar interaction would be decreased with the distortion of the phenolate rings from the planar conformation, depending on the geometric relationship between the paramagnetic metal center and the shifted nucleus, as schematically shown in Figure S8.[29] The smaller shifts for **1**-OCH_2CF_3 and **1**-N_3 as compared with **1**-NO_3 and **1**-Cl may imply **1**-OCH_2CF_3 and **1**-N_3 may adopt a stepped conformation in solution as well as in the solid state. It is also interesting to note that the extent of signal broadening for one of two *tert*-butyl groups differs depending on the external axial ligand, suggesting a different conformational equilibrium. Although the X-ray crystal structure shows **1**-Cl adopts a planar conformation with unequivalent phenolate rings, the signals for the 4/4′H and 6/6′H of the phenolate rings in **1**-Cl-*d* as well as **1**-OCH_2CF_3-*d* and **1**-N_3-*d* in a C_2-symmetric stepped conformation is not resolved even at 233 K. This is possibly because fluctuation of the phenolate rings occurs at a rate comparable to the NMR time scale. This is in clear contrast with Fox's Ni(salen) system bearing a large substituent at the 3/3′ positions, which was reported to show a chemical exchange with coalescence at 253 K.[18]

Quantum-Chemical Study of Circular Dichroism from a Salen Complex. To gain an understanding of circular dichroism and solution conformations of a salen complex, quantum-chemical calculations are carried out using the SAC-CI (symmetry adapted cluster-configuration interaction) method.[30] First, we carried out a quantum-chemical calculation for the metal-free salen ligand that is composed of (*R*,*R*)-*trans*-cyclohexane-1,2-diamine and unsubstituted salicylidene rings and compared the theoretical result with the experimental observation to confirm the validity of the present calculation. A DFT (density functional theory) calculation at the B3LYP/6-311+G(d) level of theory gives the optimized geometry (Figure S9, Supporting Information), for which SAC-CI calculations are carried out. Table 3 summarizes the calculated circular dichroism for the metal-free salen ligand. Molecular orbitals that are related to the transition are shown in Table S1 and Figure S10 (Supporting Information). The calculation indicates three sets of CD-active absorptions, which are fully consistent with the experimental observation in Figure 3. Furthermore, the present quantum-chemical calculation well reproduces the experimental wavelengths

(29) Ming, L.-J. In *Physical Methods in Bioinorganic Chemistry, Spectroscopy and Magnetism*; Que, L. , Jr., Ed.; University Science Books: CA, 2000; p 375.
(30) (a) Nakatsuji, H. *Chem. Phys. Lett.* **1978**, *59*, 362–364. (b) Nakatsuji, H. *Chem. Phys. Lett.* **1979**, *67*, 329–333.

Table 3. Calculated Circular Dichroism for the Salen Ligand with SAC−CI Calculations[a]

symmetry[b]	wavelength/nm	rotatory strength
1B	303.0	−565.2
1A	301.0	376.2
2A	252.8	45.7
2B	251.5	−41.6
3B	232.1	−217.1
3A	224.2	250.8

[a] An optimized structure of the salen ligand with a DFT calculation, for which SAC-CI calculations are carried out, is shown in Figure S9. [b] Assignment of the transitions that are responsible for the CD is shown in Table S1.

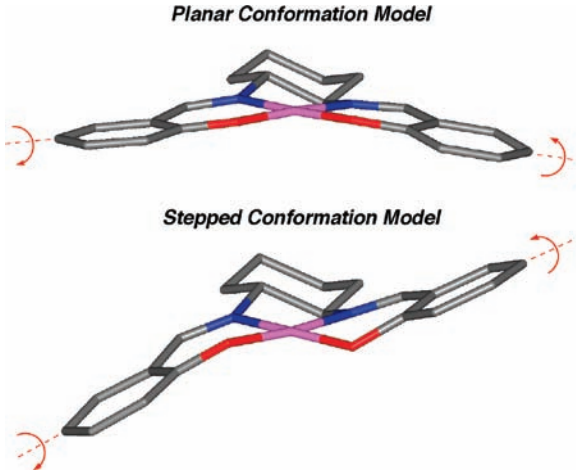

Figure 8. Planar and stepped conformations of the Ni^{II}(salen) model which is created from the X-ray structure of **1**-Cl and **1**-OCH_2CF_3, respectively. These structures are utilized for quantum chemical calculations with the SAC-CI method. The arrows indicate the directions of the twist of the phenolates to calculate CD for conformations with twisted phenolates.

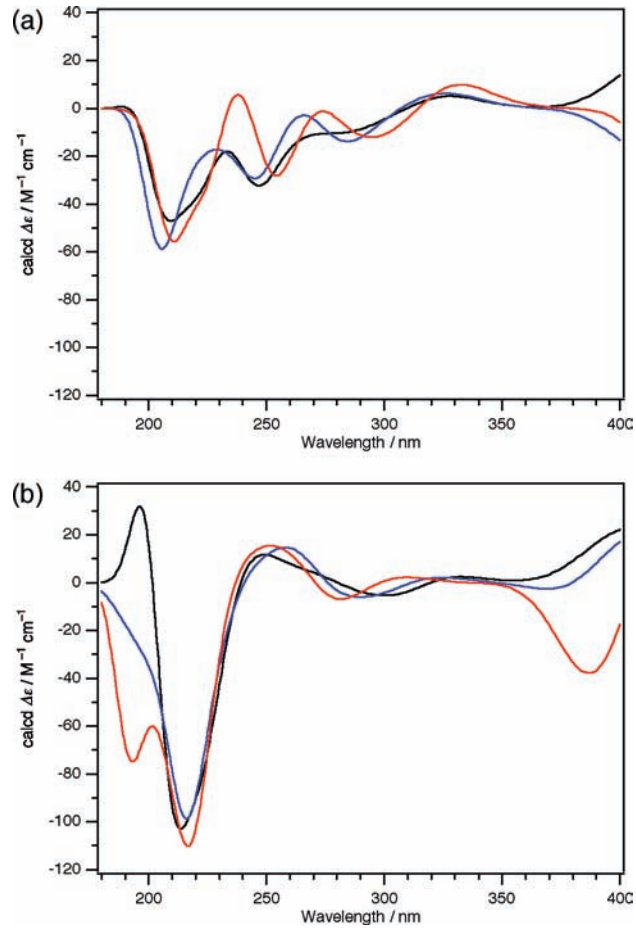

Figure 9. Calculated CD spectra for (a) the planar conformation (black line) and (b) the stepped conformation (black line) of the Ni(salen) model shown in Figure 8. Quantum-chemical calculations are also carried out for the conformations in which the phenolates are twisted to a lesser (blue line) and greater extent (red line) along one of the molecular vibration modes, as shown by the red arrows in Figure 8.

with an error of less than ∼30 nm. We also carried out a quantum-chemical calculation for hypothetical structures in which two benzene rings are placed in exactly the same manner as the stepped conformation from **1**-OCH_2CF_3 and the planar conformation from **1**-Cl (Figure S11, Supporting Information), to consider exactly what gives rise to CD from the metal-free salen ligand. Irrespective of arrangements of the benzene rings, a theoretical calculation gives no CD-active absorption, indicative of an important role of the azomethine moiety for relatively strong CD from the salen ligand. This theoretical result well accounts for the experimental observation that the tetrahydrosalen ligand, (*R*,*R*)-**3**, without the azomethine moiety exhibits only weak CD as compared to the salen ligand, (*R*,*R*)-**1** (Figure 3).

We then carried out quantum-chemical calculations for circular dichroism from planar and stepped conformation models in which Mn is replaced by Ni for ease of computation (Figure 8). As shown in Figure 9, the stepped conformation model created from the X-ray structure of **1**-OCH_2CF_3 exhibits more intense CD than the planar conformation model that is created from **1**-Cl in the range 180−300 nm (depicted in a black line). These CD bands are attributed to transitions associated with the salen ligand. We further consider a possibility that the calculated CD intensity may reflect a twist of the phenolates, rather than the difference between the planar and stepped conformations. Then, CD spectra are also calculated for the conformations in which the phenolates are twisted along one of the molecular vibration modes as shown by red arrows in Figure 8. Even though the planar conformation model is altered from the starting conformation (black line) to those with twisted phenolates to a lesser (blue line) and greater extent (red line), the CD from the planar conformation model remains weaker than the CD from the stepped conformation model (Figure 9). Therefore, it is securely indicated that a metal salen complex in a stepped conformation exhibits substantially more intense CD than a metal salen complex in a planar conformation.

Discussion

Biologically important chiral structural motifs such as helices of DNA and proteins are built up from asymmetric carbon atoms of point chirality. Therefore, synthetic molecules with such higher-order chirality has been of great interest and extensively studied from both fundamental and practical viewpoints.[31] It has been shown that noncovalent interactions such as hydrogen bonding play an important role to create and maintain such higher-order chirality. In the case of Jacobsen's salen complexes, the formation of a chiral conformation, if any, is similarly directed by the asymmetric carbon atoms in *trans*-cyclohexane-1,2-diamine as the only chiral unit. However, Jacobsen's salen complexes apparently lack such noncovalent interactions that could support a chiral conformation, according to the previous design criteria. In addition, Fox et al. rigorously investigated

solid-state and solution conformations of their well-designed Ni^{II}(salen) complexes and unambiguously showed that *trans*-cyclohexane-1,2-diamine is only a weak director to induce a chiral conformation in a metal salen complex.[18] Thus, there has been a good reason to assume that Jacobsen's salen complex may not adopt a distinct chiral conformation in solution, although exquisite enantioselectivity by Jacobsen's salen complexes has been frequently ascribed to a chiral conformation of some kind or another.[2f]

We show herein that the solution of **1**-L exhibits CD of increasing intensity in the order $L = Cl < NO_3 \ll N_3 < OCH_2CF_3$ in the range 200−300 nm (Figure 5). Because UV−vis spectra in this region do not differ to any significant extent (Figure 4), the CD bands of different intensity cannot be a result of an overlap with additional CD upon substitution of the axial ligands L but are securely attributed to a conformational difference. It is thus indicated **1**-L adopts a solution conformation of an increasing chiral distortion depending on the axial ligands in this order. In accordance with the observation from CD spectroscopy, ^{2}H NMR spectroscopy also indicates a difference of solution conformations similarly depending on the external axial ligands. The most remarkable structural difference in **1**-L is a Mn−L bond length, which becomes shorter in parallel with the degree of a chiral distortion in the order L = Cl (2.263−2.300 Å) > N_3 (1.958−2.006 Å)[23] > OCH_2CF_3 (1.866−1.880 Å), while the other structural parameters such as $Mn-O_{salen}/N_{salen}$ bond lengths are not altered. The order of a chiral distortion in **1**-L is also in parallel with the pK_a values of HL (HCl, −7;[32] HNO_3, −1.4;[32] HN_3, 4.72;[33] CF_3CH_2OH, 11.4[34]), which reflect the ability of L^- to dissociate in solution. These observations indicate a rather unexpected finding that the formation of a chirally distorted conformation is significantly facilitated by external axial ligands that could coordinate to the Mn center from both sides along the axial direction with a shorter Mn−L bond length and a lower degree of dissociation in solution. In light of the present finding, a failure to form a chirally distorted conformation in five-coordinate and four-coordinate metal salen complexes such as Mn^{III}(salen)(L)[23] and Ni^{II}(salen)[18] as reported previously might be ascribed to the absence of such external axial ligands. Although we could not obtain definitive evidence for solution conformations, **1**-OCH_2CF_3, **1**-N_3,[23] and **2**-N_3 exhibiting more intense CD are crystallized as a stepped conformation without exception, while the crystal of **1**-Cl exhibiting relatively weak CD contains a planar conformation. In addition, quantum-chemical calculations indicate that a stepped conformation exhibits more intense CD than a planar conformation. Therefore, a chirally distorted conformation that is formed in the solution of **1**-L more preferentially in the order $L = Cl < NO_3 \ll N_3 < OCH_2CF_3$ would be most probably a stepped conformation.[25]

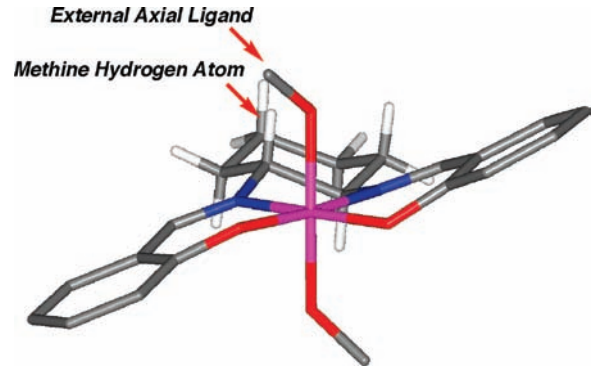

Figure 10. A model that is reproduced from the X-ray crystal structure of **1**-OCH_2CF_3.

One possible explanation for the role of axial ligands is steric repulsion between the *trans*-cyclohexane-1,2-diamine moiety as the only chiral center and the axial ligands coming close to the Mn center, which bring the axial ligands to one asymmetric direction and then puts down the salicylidene rings. As shown in Figure 10, the methine hydrogen atom of *trans*-cyclohexane-1,2-diamine, which is closest to the axial ligands, is considered the most important steric factor. But the methine hydrogen atom is expected to rather bring the OCH_2CF_3 or N_3 group to the direction that disturbs the formation of a stepped conformation, and hence the possibility of steric repulsion is ruled out. It is also interesting to note that **2**-N_3 bearing much less sterically demanding salicylidene rings similarly adopts a chirally distorted conformation in solution, which means steric interaction between the external axial ligand and the *tert*-butyl groups is not a major factor for chiral distortion. Our hypothesis from the present work is that tight binding of the external axial ligands from both sides along the axial direction confines the movement of the Mn ion along this direction, which may serve to enhance the energy difference among conformers. In the case of tightly bound ligands such as OCH_2CF_3 and N_3, the stability of the stepped conformation might be significantly enhanced, leading to an increased distribution of this conformer relative to the others in solution, which results in the appearance of intense circular dichroism and also crystallization exclusively as a stepped conformer. In the case of weakly bound ligands such as NO_3 and Cl, the energy difference among conformers remains very small, and then the solution of salen complexes bearing such axial ligands contains an almost equimolar mixture of multiple conformers, which could account for the circular dichroism of low intensity even at lower temperatures and broadened ^{2}H NMR signals.

Conclusion

We herein prepare a series of Mn^{IV}(salen)$(L)_2$ complexes bearing different external axial ligands (L) from Jacobsen's salen ligand and clarify a rather unexpected finding that the external axial ligands play a pivotal role in effectively transmitting the chirality at the bridging diamine moiety to the phenolate moiety.

(31) For example, see: (a) Mizutani, T.; Yagi, S.; Morinaga, T.; Nomura, T.; Takagishi, T.; Kitagawa, S.; Ogoshi, H. *J. Am. Chem. Soc.* **1999**, *121*, 754–759. (b) Inai, Y.; Tagawa, K.; Takasu, A.; Hirabayashi, T.; Oshikawa, T.; Yamashita, M. *J. Am. Chem. Soc.* **2000**, *122*, 11731–11732. (c) Kurtán, T.; Nesnas, N.; Koehn, F. E.; Li, Y.-Q.; Nakanishi, K.; Berova, N. *J. Am. Chem. Soc.* **2001**, *123*, 5974–5982. (d) Kano, K.; Hasegawa, H. *J. Am. Chem. Soc.* **2001**, *123*, 10616–10627. (e) Lintuluoto, J. M.; Borovkov, V. V.; Inoue, Y. *J. Am. Chem. Soc.* **2002**, *124*, 13676–13677. (f) Maeda, K.; Morino, K.; Okamoto, Y.; Sato, T.; Yashima, E. *J. Am. Chem. Soc.* **2004**, *126*, 4329–4342. (g) Yu, J.; RajanBabu, T. V.; Parquette, J. R. *J. Am. Chem. Soc.* **2008**, *130*, 7845–7847.

(32) Bell, R. P. *The Proton in Chemistry*, 2nd ed.; Cornel University Press: Ithaca, NY, 1973.

(33) Bjerrum, J.; Schwarzenbach, G.; Sillén, L. G. *Stability Constants of Metal-Ion Complexes*; Chemical Society: London, 1958.

(34) Ballinger, P.; Long, F. A. *J. Am. Chem. Soc.* **1959**, *81*, 1050–1053.

The present new finding would provide valuable insight to create metal salen complexes with unique stereochemical properties.

Experimental Section

Caution! All the operations for preparing **1**-Cl, including filtration of the product, should be carried out in a fume hood. A volatile substance, probably Cl_2, which is generated during the preparation, causes serious damage to eye, nose, and mouth.

Instrumentation. UV−vis spectra were recorded in spectrophotometric grade CH_2Cl_2 in a quartz cell ($l = 0.1$ cm) on an Agilent 8453 spectrometer (Agilent Technologies) equipped with a USP-203 low-temperature chamber (UNISOKU). CD spectra were recorded in a quartz cell ($l = 0.1$ cm) on a J-720W spectropolarimeter (JASCO) equipped with a USP-203 low-temperature chamber (UNISOKU). Measurements were done under the following conditions: scan rate, 100 nm min^{-1}; bandwidth, 5.0 nm; response, 4 s; resolution, 1 nm. EPR spectra were recorded for 30 μL of the 10 mM solution in a quartz cell ($d = 5$ mm) on an E500 continuous wave X-band spectrometer (Bruker) with an ESR910 helium-flow cryostat (Oxford Instruments). Measurements were made under the following conditions: microwave frequency, 9.56 GHz; microwave power, 2.012 mW; modulation amplitude, 7 G; time constant, 163.84 ms; conversion time, 163.84 ms. 500 and 400 MHz NMR spectra were measured on an LA-500 and LA-400 spectrometer (JEOL), respectively. ^{1}H NMR chemical shifts in CD_2Cl_2 and $CDCl_3$ were referenced to $CHDCl_2$ (5.32 ppm) and $CHCl_3$ (7.24 ppm), respectively. ^{13}C NMR chemical shifts in $CDCl_3$ were reported relative to $CHCl_3$ (77.0 ppm). Elemental analyses were conducted on a CHN corder MT-6 (Yanaco). High-resolution mass spectra were measured with the JMS-777 V mass spectrometer (JEOL).

X-ray Crystallography. Measurements were made on a Rigaku/MSC Mercury CCD diffractometer equipped with graphite monochromated Mo Kα radiation ($\lambda = 0.710\,70$ Å). Data were collected at 93 K under a cold nitrogen stream. All crystals were mounted on a glass fiber using epoxy glue. The images were processed with the CrystalClear program (ver. 1.3.5).[35] The structures were solved by the direct method using SHELXS-97[36,37] and refined by full-matrix least-squares procedures on F^2 using SHELXL-97,[36,38] with the CrystalStructure software package (ver. 3.8.2).[39] Anisotropic refinement was applied to all nonhydrogen atoms. Hydrogen atoms were placed at the calculated positions and refined with isotropic parameters. Corrections for Lorentz polarization effects and absorption were performed. The Flack parameters[40] were calculated to confirm the absolute configuration. In the case of **1**-OCH_2CF_3, one of four *tert*-butyl groups was disordered and was treated as such during the refinement procedure. The Checkcif program gives an A-level alert to suggest another space group, $P\bar{1}$, for **1**-Cl, but this was confirmed not true because **1**-Cl bearing the (*R*,*R*)-*trans*-cyclohexane-1,2-diamine moiety is incompatible with an inversion center. The Checkcif program points an A-level alert on a suspected C−H bond for **1**-OCH_2CF_3, but this is an artifact of the disordered *tert*-butyl group. The structural parameters including α, β, and the Mn−N_2O_2−plane distance were obtained using the crystal structure visualization and exploration program, Mercury (ver. 2.2), provided by the Cambridge Crystallographic Data Center.

Quantum-Chemical Calculations. Quantum-chemical calculations were performed using the Gaussian03 program package.[41] The optimized structures were calculated using the B3LYP/6-311+G(d) level of theory. Circular dichroism was calculated with the SAC-CI method.

Materials. Anhydrous and spectrophotometric grade CH_2Cl_2 and other anhydrous solvents were purchased from Kanto or Wako and were utilized as received. CD_2Cl_2 and $CDCl_3$ were purchased from ACROS and were passed though aluminum oxide just before use. NaH (65% dispersion in mineral oil) was purchased from Wako. $NaBH_4$ was purchased from Nacalai. $AgNO_3$ (99.9999%), CF_3CH_2OH (99.5%), (*R*,*R*)-/(*S*,*S*)-*N*,*N*′-bis(3,5-di-*tert*-butylsalicylidene)-1,2-cyclohexanediaminomanganese(III) chlorides, and $ReBr(CO)_5$ were purchased from Aldrich and were used as received. *m*-CPBA (*m*-choloroperoxybenzoic acid) was purchased from Nacalai and purified by washing with phosphate buffer. The purity of *m*-CPBA was checked with iodometry. (*R*,*R*)-1,2-Cyclohexanediamine and 5-methylsalicylaldehyde were purchased from Tokyo Chemical Industry and utilized as received. Manganese(II) acetate tetrahydrate was purchased from Wako. Phenol-d_6 (98%) was purchased from Cambridge Isotope Laboratories, Inc.

Synthesis of (*R*,*R*)-3. To the solution of (*R*,*R*)- or (*S*,*S*)-**1** (1 g, 1.83 mmol) in anhydrous tetrahydrofuran (8 mL) and anhydrous methanol (8 mL) were added 10 equiv of $NaBH_4$ (691.8 mg, 18.3 mmol) at 273 K. The resulting solution was stirred at room temperature for 3 h, and then the solvent was removed by rotary evaporation. The residue was dissolved in CH_2Cl_2 (100 mL). The organic layer was washed with distilled water (50 mL × 3) and then a saturated NaCl aqueous solution (50 mL × 1). The organic layer was dried over anhydrous $MgSO_4$. The solvent was removed by rotary evaporation, and the residue was purified by recrystallizing from hot methanol to give (*R*,*R*)- or (*S*,*S*)-**3** (540 mg, 0.98 mmol) in 54% yield as a colorless crystalline solid: ^{1}H NMR (400 MHz, $CDCl_3$) δ 1.2−1.3 (m, 4H), 1.27 (s, 18H), 1.36 (s, 18H), 1.6−1.8 (m, 2H), 2.1−2.3 (m, 2H), 2.4−2.6 (m, 2H), 3.96 (AB, $J = 13.6$ Hz, 4H), 6.85 (d, $J = 2.4$ Hz, 2H), 7.19 (d, $J = 2.4$ Hz, 2H), 10.6 (brs, 2H); ^{13}C NMR (100.4 MHz, $CDCl_3$) δ 24.1, 29.6, 30.7, 31.7, 34.1, 34.8, 50.8, 59.9, 122.3, 123.0, 123.1, 136.0, 140.6, 154.4; HRMS (FAB) *m*/*z* calcd for $C_{36}H_{59}N_2O_2$ $[M + H]^+$ 551.4577, found 551.4570. Anal. Calcd for $C_{36}H_{58}N_2O_2$: C, 78.49; H, 10.61; N, 5.09. Found: C, 78.51; H, 10.67; N, 5.09.

Synthesis of 1-Cl. The stream of O_3 and O_2 prepared by UV-irradiation to the O_2 gas was passed through a solution of Mn^{III}(salen)(Cl) from (*R*,*R*)-**1** (200 mg, 0.31 mmol) in anhydrous CH_2Cl_2 (7 mL) at 193 K. After 1.5 h, the cold solution was filtered and the filtrate was stirred at room temperature for 20 min. Anhydrous pentane (90 mL) was added to the filtrate, and then the resulting solution was stirred at 233 K for 10 min to give a green precipitate. This was filtered off, washed with pentane, and dried *in vacuo*. Recrystallization from CH_2Cl_2 (2 mL) and pentane (50 mL) at 253 K gave analytically pure **1**-Cl (82 mg, 0.12 mmol) in 39% yield. The crystal suitable for the X-ray crystallographic analysis was obtained by crystallizing **1**-Cl (10 mg) in CH_2Cl_2 (0.5 mL) and pentane (10 mL) at 253 K. Anal. Calcd for $C_{36}H_{52}Cl_2MnN_2O_2\cdot(H_2O)_{0.2}$: C, 64.13; H, 7.83; N, 4.15. Found: C, 64.11; H, 7.65; N, 4.25.

Synthesis of 1-NO_3. To the solution of **1**-Cl (112.3 mg, 0.167 mmol) in anhydrous CH_2Cl_2 (4 mL) were added 10 equiv of $AgNO_3$ (284.4 mg, 1.67 mmol) at 233 K. The resulting solution was stirred for 3 h at 233 K. Then, the cold solution was filtered to remove silver salts, and the cold filtrate kept at 233 K was passed through a membrane filter (Cosmonice Filter S, pore size 0.45 μm, diameter 13 mm, Nacalai). Anhydrous pentane (50 mL) was added to the

(35) (a) *CrystalClear 1.3.5 SP2*; Rigaku and Molecular Structure Corp.: The Woodlands, TX, 2004. (b) Pflugrath, J. W. *Acta Crystallogr.* **1999**, *D55*, 1718–1725.
(36) Sheldrick, G. M. *Acta Crystallogr.* **2008**, *A64*, 112–122.
(37) Sheldrick, G. M. *SHELXS-97, Program for Crystal Structure Solution*; University of Göttingen: Göttingen, Germany, 1997.
(38) Sheldrick, G. M. *SHELXL-97, Program for Refinement of Crystal Structures*; University of Göttingen: Göttingen, Germany, 1997.
(39) (a) *CrystalStructure 3.8.2: Crystal Structure Analysis Package*, version 3.8.2; Rigaku and Rigaku/MSC: The Woodlands, TX, 2007. (b) Watkin, D. J.; Prout, C. K.; Carruthers, J. R.; Betteridge, P. W. *Crystals, Issue 10*; Chemical Crystallography Laboratory: Oxford, U.K., 1996.
(40) Flack, H. D. *Acta Crystallogr.* **1983**, *A39*, 876–881.
(41) Frisch, M. J. *Gaussian03*, revision C.03; Gaussian, Inc.: Wallingford, CT, 2004.

filtrate at 233 K to give a green precipitate. This was filtered off, washed with pentane, and dried *in vacuo*. Recrystallization from CH_2Cl_2 (2 mL) and pentane (20 mL) at 253 K gave analytically pure **1**-NO_3 (39.5 mg, 0.055 mmol) in 33% yield. Anal. Calcd for $C_{36}H_{52}MnN_4O_8\cdot(H_2O)_{1.5}$: C, 57.59; H, 7.38; N, 7.46. Found: C, 57.34; H, 7.02; N, 7.56.

Synthesis of 1-OCH_2CF_3. To a solution of Mn^{III}(salen)(Cl) from (*R*,*R*)-**1** (495.5 mg, 0.78 mmol) in anhydrous CH_2Cl_2 (20 mL) was added 1.0 equiv of *m*-CPBA (134.6 mg, 0.78 mmol) at 233 K. After the mixture was stirred for 30 min, 3 equiv of NaH (65% dispersion in mineral oil, 86.4 mg, 2.34 mmol) dissolved in CF_3CH_2OH (2 mL) were added to the reaction mixture at 233 K. After the mixture was stirred for 1 h at 233 K, the solvent was removed *in vacuo* at 253 K. The resulting solid was dissolved in CH_2Cl_2 (10 mL) at room temperature, and the solution was filtered through a filter paper and then a membrane filter (Millex-FG, pore size 0.20 μm, diameter 25 mm, Millipore). The solvent was removed by rotary evaporation. The residue was dissolved in a small amount of CH_2Cl_2−pentane (1:10), and the addition of pentane (∼100 mL) at 233K gave analytically pure **1**-OCH_2CF_3 (384 mg, 0.48 mmol) in 62% yield as a reddish precipitate. Crystals suitable for the X-ray crystallographic analysis were obtained by crystallizing **1**-OCH_2CF_3 (10 mg) in CH_3CN (4 mL) at 253 K. Anal. Calcd for $C_{40}H_{56}F_6MnN_2O_4$: C, 60.22; H, 7.07; N, 3.51. Found: C, 60.04; H, 7.00; N, 3.63.

Synthesis of (*R*,*R*)-*N*,*N*′-Bis(5-methylsalicylidene)-1,2-cyclohexanediamine. 5-Methylsalicylaldehyde (11.35 g, 83.4 mmol) in anhydrous EtOH (80 mL) was heated to reflux (∼363 K) until dissolution was achieved, and then (*R*,*R*)-1,2-cyclohexanediamine (4.76 g, 41.7 mmol) dissolved in anhydrous EtOH (20 mL) was added. The resulting solution was stirred at reflux (∼363 K) for 1 h, and then the solution was cooled at 277 K to give a yellow precipitate. The precipitate was collected by vacuum filtration and dried in vacuo at 373 K. The product was obtained as a yellow powder in 77% yield (11.24 g, 32.1 mmol). ^{1}H NMR (400 MHz, $CDCl_3$) δ 1.4−2.0 (m, 8H), 2.19 (s, 6H), 3.2−3.3 (m, 2H), 6.77 (d, J = 8.4 Hz, 2H), 6.91 (d, J = 1.6 Hz, 2H), 7.02 (dd, J = 1.6, 8.4 Hz, 2H), 8.18 (s, 2H), 13.07 (s, 2H); ^{13}C NMR (100.4 MHz, $CDCl_3$) δ 20.2, 24.1, 33.1, 72.7, 116.4, 118.3, 127.6, 131.5, 132.8, 158.6, 164.6; HRMS (FAB) *m*/*z* calcd for $C_{22}H_{27}N_2O_2$ $[M + H]^+$ 351.2073, found 351.2065. Anal. Calcd for $C_{22}H_{26}N_2O_2$: C, 75.40; H, 7.48; N, 7.99. Found: C, 75.54; H, 7.57; N, 7.99.

Synthesis of (*R*,*R*)-*N*,*N*′-Bis(5-methylsalicylidene)-1,2-cyclohexanediaminomanganese(III) Chloride. (*R*,*R*)-*N*,*N*′-Bis(5-methylsalicylidene)-1,2-cyclohexanediamine (5.00 g, 14.3 mmol) in anhydrous EtOH (40 mL) was heated to reflux (363 K) until dissolution was achieved, and then manganese acetate tetrahydrate (10.49 g, 42.8 mmol) was added. The resulting mixture was stirred at reflux for 1 h, and then the solvent was removed by rotary evaporation. The residue dissolved in CH_2Cl_2 (300 mL) was washed with 1 M HCl (100 mL × 3) and brine (100 mL × 1). After drying over $MgSO_4$, the solvent was removed by rotary evaporation. To the residue redissolved in CH_3OH was added a 1 M HCl aqueous solution to give a precipitate. The precipitate was collected by vacuum filtration and dried in vacuo at 373 K. The product was obtained as a brown powder in 39% yield (2.46 g, 5.61 mmol). Anal. Calcd for $C_{22}H_{24}ClMnN_2O_2$: C, 60.21; H, 5.51; N, 6.38. Found: C, 60.18; H, 5.47; N, 6.40.

Synthesis of 2-N_3. To a solution of (*R*,*R*)-*N*,*N*′-bis(5-methylsalicylidene)-1,2-cyclohexanediaminomanganese(III) chloride (201.6 mg, 0.459 mmol) dissolved in anhydrous CH_2Cl_2 (10 mL) and anhydrous CH_3OH (10 mL) was added 1 equiv of *m*-CPBA (75%, 105.7 mg, 0.459 mmol) at 233 K. After the mixture was stirred for 1 h at 233 K, 10 equiv of NaN_3 (298.7 mg, 4.59 mmol) in H_2O (1 mL) were added. The resulting solution was stirred at 233 K for 1 h, and then the solvent was removed in vacuo at 253 K. The residue dissolved in CH_2Cl_2 (10 mL) at 233 K was passed through a pad of Celite and subsequently through a membrane filter (Millex-FG, pore size 0.20 μm, diameter 25 mm, Millipore). Addition of anhydrous pentane (10 mL) at 233 K gave a green precipitate. The product was redissolved in CH_2Cl_2 (10 mL) at 233 K and was precipitated by the addition of pentane (8 mL). Precipitation from CH_2Cl_2 (10 mL) and pentane (8 mL) was repeated three times. The precipitate was collected by vacuum filtration and dried in vacuo at room temperature. The product was obtained as a green powder in 21% yield (46.6 mg, 0.096 mmol). Anal. Calcd for $C_{22}H_{24}MnN_8O_2\cdot(CH_3OH)_{0.3}$: C, 53.89; H, 5.11; N, 22.54. Found: C, 54.30; H, 5.02; N, 22.10.

Scheme 2

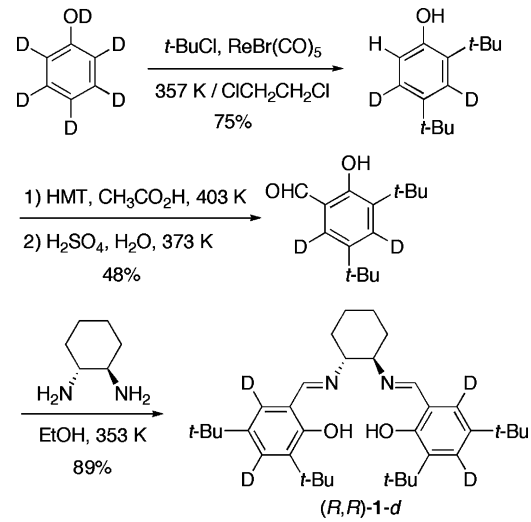

Synthesis of 2,4-Di-*tert*-butylphenol-*d*. Preparation of ^{2}H-labeled Jacobsen's salen ligand, (*R*,*R*)-**1**-*d*, is outlined in Scheme 2. 2,4-Di-*tert*-butylphenol-*d* was synthesized from commercially available phenol-d_6 according to the procedure of Nishiyama and Sonoda[42] with a slight modification to the amount of *t*-BuCl to improve the yield of the desired product. $ReBr(CO)_5$ (51.3 mg, 0.13 mmol) and *t*-BuCl (6.8 mL, 62.5 mmol) were added to a solution of phenol-d_6 (1.25 g, 12.5 mmol) in 1,2-dichloroethane (23 mL). The resulting mixture was stirred at 357 K for 30 min, and then the solvent was removed by rotary evaporation. The residue was purified by silica flash column chromatography (CH_2Cl_2/hexane = 2:5) to give 2,4-di-*tert*-butylphenol-*d* (1.95 g, 9.4 mmol) in 75% yield as a viscous oil. ^{1}H NMR and mass spectrometry indicate 90% of the ^{2}H at the ortho position and 20% of the ^{2}H at the meta position were replaced with ^{1}H under the reaction conditions (Figure S12, Supporting Information).

Synthesis of 3,5-Di-*tert*-butyl-2-hydroxybenzaldehyde-*d*. The procedure of Jacobsen and Gao[43] was employed except for the purification step. 2,4-Di-*tert*-butylphenol-*d* (1.71 g, 8.2 mmol) and hexamethylenetetramine (HMT, 2.30 g, 16.4 mmol) in glacial acetic acid (4 mL) were heated at 403 K for 3 h. 33% (w/w) aqueous H_2SO_4 (4 mL) was added to the mixture at 373 K, and the mixture was stirred at this temperature for 1 h. The resulting mixture was allowed to cool to room temperature and extracted with diethyl ether (150 mL). The extract was washed with brine (100 mL × 3) and then dried over $MgSO_4$. The solvent was removed by rotary evaporation. The crude product was purified by silica flash column chromatography (CH_2Cl_2/hexane = 1:4) to give 3,5-di-*tert*-butyl-2-hydroxybenzaldehyde-*d* (940 mg, 4 mmol) in 48% yield as a pale-yellow solid. ^{1}H NMR and mass spectra show the ^{2}H atoms that are incorporated at the meta position of the phenolate rings remain intact under the reaction conditions (Figure S13, Supporting Information).

(42) Nishiyama, Y.; Kakushou, F.; Sonoda, N. *Bull. Chem. Soc. Jpn.* **2000**, *73*, 2779–2782.
(43) Larrow, J. F.; Jacobsen, E. N.; Gao, Y.; Hong, Y.; Nie, X.; Zepp, C. M. *J. Org. Chem.* **1994**, *59*, 1939–1942.

Synthesis of (*R*,*R*)-1-*d*. (1*R*,2*R*)-1,2-Diaminocyclohexane (225.3 mg, 1.97 mmol) in EtOH (5 mL) was added to a solution of 3,5-di-*tert*-butyl-2-hydroxybenzaldehyde-*d* (932.5 mg, 3.95 mmol) in EtOH (30 mL). The resulting mixture was heated at 353 K for 1 h and then allowed to cool to room temperature. The precipitate was collected by vacuum filtration and dried in vacuo at 353 K. The product was obtained as a yellow solid in 89% yield (965.2 mg, 1.75 mmol). ^{1}H and ^{2}H NMR spectroscopy shows ^{2}H was incorporated to the phenolate rings (80% D) as well as the *tert*-butyl groups (7% D) (Figure S7, Supporting Information). ESI-MS spectrometry shows the product contains a mixture of molecules that are labeled with 2 to 8 ^{2}H atoms (Figure S7, Supporting Information).

Acknowledgment. We thank Mr. Seiji Makita (IMS) for elemental analysis and measurements of high-resolution mass spectrometry. This work was supported by grants from the Japan Science and Technology Agency, CREST and the Japan Science Promotion Society, the Global COE program.

Supporting Information Available: The X-ray crystallographic file in the CIF format for **1**-Cl, **1**-OCH_2CF_3, and **2**-N_3. Figures S1−S13, Table S1, and complete ref 41. This material is available free of charge via the Internet at http://pubs.acs.org.

JA904635N